LAWRENCE
LIVERMORE
NATIONAL
LABORATORY

UCRL-JRNL-230135

CAMS/LLNL Ion Source Efficiency Revisited

S. J. Fallon, T. P. Guilderson, T. A. Brown

April 20, 2007

Nuclear Instruments and Methods in Physics Research B

CAMS/LLNL Ion Source Efficiency Revisited

Stewart J. Fallon, Thomas P. Guilderson, Thomas A. Brown

Center for Accelerator Mass Spectrometry, Lawrence Livermore National Laboratory, Livermore, Ca. 94550

Abstract

The Center for AMS, Lawrence Livermore National Laboratory (CAMS) modified high-intensity Cs^+ sputter source has several key characteristics, including very high ion current output, that make it useful for AMS applications. Within the AMS community there have been suggestions that certain aspects of operation of a sputter ion source at very high output levels could result in low ionization efficiency and the likelihood of consuming (burning through) small samples without acquiring adequate statistics. This is of particular importance for small mass carbon targets. We have recently re-determined the carbon ionization efficiency of the CAMS sputter source using graphite targets derived from Oxalic Acid I & II and demonstrated relatively high ionization efficiency (~33%) during the operation of these sources at high output levels. We also examine the relationship between ion source efficiency and sample size.

Keywords: AMS, ion source, efficiency

1. Introduction

The CAMS ion source underwent a significant overhaul/evolution from the original General Ionex Corp. Model 486 high-intensity multi-sample source from 1989-1999. The modifications resulted in improved reliability, increased output and reduced sample memory, and are discussed in detail by Southon and Roberts [1]. In brief, the sample chamber was completely redesigned with proper shielding of insulators, the high voltage

gap clearances were increased and the source body and sample wheel were constructed of stainless steel. The vacuum in the source and injection lines was greatly improved by increasing distances between the ionizer assembly and immersion lens as well as adding a 2000l/s CTI Cryo-Torr 8 pump. Better thermal isolation of the ionizer assembly was achieved resulting in lower power consumption by the ionizer and a decrease in thermal loading on the source body. Higher cathode voltages were enabled by the installation of extraction and cathode insulator shields. A six-hole Cs-feed shroud, producing six Cs vapor jets aimed at the spherical ionizer surface, was also implemented. The increase in source performance due to these modifications has been studied by ion source modeling [2]. In this study we re-examine and attempt to quantify the efficiency of the CAMS source using Oxalic Acid I (OX-I) and Oxalic Acid II (OX-II) targets containing known ^{14}C quantities over the course of multiple experimental sample runs. We then compare the derived ionization and total system (ionization and transmission) efficiencies to the potential efficiency of gas-based ion sources for ^{14}C AMS.

2. Methods

Aliquots of oxalic acid and copper oxide were loaded into quartz tubes, evacuated, and combusted following standard protocols. The produced OX-I and OX-II CO_2 was converted to graphite using iron catalyst following a method similar to that described by Vogel et al. [3]. Each graphite target contained ~ 1 mg of C. The targets were analyzed using the CAMS modified high intensity Cs sputter ion source and HVEC Model FN Van de Graaff accelerator-based AMS system. The geometry and target location of the CAMS source are optimized to sputter the surface of the target graphite-catalyst matrix at

a position just beyond the cesium focal point, which results in the sputtering being concentrated in an annular ring centered within the sample well with a less-sputtered cone in the middle of the target well. This optimized positioning of the samples exposed more of the sample to the sputtering Cs^+ ions than would occurred if the samples had been positioned forward at the Cs^+ ion beam waist. We collected ^{14}C data in blocks of 50-100 k counts or 200 s, whichever was shorter. The graphite targets were run to "exhaustion"; i.e., the targets were analyzed until $^{13}C^{4+}$ currents fell from the initial 5-7 μA range to less than ~0.3 μA. Efficiency experiments were run on 3 separate occasions, Nov. 15, 2003, Jul. 7 and Jul. 31, 2005.

In order to determine the total system and ionization efficiencies we used the known $^{14}C/^{12}C$ atom ratios of OX-I and OX-II, 1.2 X 10^{-12} [4] and 1.5 X 10^{-12} (calculated using the accepted OX-II to OX-I ratio of 1.293 [5]) respectively, to calculate the initial ^{14}C contents of the samples. Typical (~1mg carbon) samples of OX-I and OX-II contained ~6 x 10^7 ^{14}C atoms and ~8 x 10^7 ^{14}C atoms, respectively. To determine the total system efficiency, we compared the estimated initial ^{14}C atoms for each sample to the total ^{14}C "events" counted in the gas ionization detector for each sample. To determine ionization efficiency from the total system efficiency we had to determine the total transmission efficiency. This was accomplished by measuring the $^{12}C^-$ current at the entrance to the accelerator and the $^{12}C^{+4}$ particle current after the accelerator, the $^{12}C^-$ current was limited so as to not destroy the accelerator. The total transmission efficiency at 6.5 MeV is 48% (Table 1), this includes stripper foil (4 μg cm^{-2} carbon foil) C^- to C^{+4} charge conversion and LE/HE tube transport efficiency (e.g., loses due to residual gas charge

exchange within the tubes) and the transmission efficiency of the gridded lens at the entrance of the Dowlish Spiral Inclined tubes which is 90% [6]. Taking into account the losses at the gridded lens the C^- to C^{+4} charge conversion is 53%. Typical source operating settings are shown in Table 2.

3. Results and Discussion

A total of 8 graphite cathodes (5 OX-I, 3 OX-II) were analyzed; the results obtained are reported in Table 3.

3a. Primary Current ($^{13}C^{4+}$ μA)

In general, the primary analyzed current ($^{13}C^{4+}$ μA) tended to increase slowly at the beginning of the experiments and level off for the first hour (Figure 1). This was not the case during our first experiment (11/15/03) where the current began to drop after the first 30 min. In this experiment we analyzed only one sample and for the first 80 minutes did so in continuous blocks of 50 k ^{14}C counts. Under these conditions, we believe the sample heated up much faster than under our normal operating cycling, and the resulting higher temperature of the sample impacted the C^- emission level from the sample. After the first 80 minutes of the experiment, we changed the measurement pattern and occasionally cycled the sample out, moved briefly to sputter another sample, and then returned to sputtering the main sample. This cycling pattern resulted in the "saw tooth" pattern seen for the Nov. 15, 2003 sample in Figure 1. We infer that the cooling of the sample during non-measurement periods is the cause of the increased primary currents observed when sputtering of the sample was recommenced.

In the 7 measurements in 2005, the cathodes were cycled back and forth, as under our normal operational cycling, providing ample time between acquisition periods for the samples to cool significantly. For these 7 samples the precipitous drops in primary current near the 5000 s mark (Figure 1) probably reflect the point at which the Cs^+ ions sputtered through the bottom of the deeper annular sputtering ring and began to sputter the underlying aluminum cathode. The continued lower level primary current output reflects the continued sputtering of the remaining carbon in the central cone and the outer ring surrounding the annular ring. For the 7 samples, the primary current had fallen to very low levels (~0.3 μA) after about 15000 s, at which point essentially all of the sample material had been sputtered from the sample well. We believe that the sample positioning and resulting sputter pattern allows for significantly more efficient utilization of the total available sample than would be achieved if the samples were positioned to produce the smallest possible Cs^+ sputter spot.

3b. ^{14}C Gated Events (Counts)

Figure 2 shows the cumulative ^{14}C counts acquired over time for all 8 samples measured with the total ^{14}C counts collected from each sample listed in the legend. During the first hour of the measurements on July 31, 2005, the count rates for the OX-I and OX-II samples were ~1150 cps and ~1500 cps, respectively. At these count rates ~1 x 10^6 ^{14}C counts would be obtained from a modern sample within 15 minutes. It is interesting to note that approximately the same number of ^{14}C counts was obtained from the Nov. 15, 2003 OX-I sample as from the later 2005 OX-I samples even though the Nov. 15, 2003 samples was measured in the different above-mentioned mode and ran for twice as long as the later samples (30 k s versus 15 k s).

3c. Raw Ratios

Figure 3 shows the "raw" ^{14}C counts per nanocoulomb $^{13}C^{4+}$ obtained from the samples measured during the July 7, 2005 experiment. In general the raw isotopic ratios remain relatively constant throughout the life of the samples, although there are some fluctuations in the ratio when the samples are nearly exhausted. In the first experiment (Nov. 15, 2003 – not shown in Figure 3) the ratios fluctuated when the primary current dropped; we attribute this to the extreme heating of the cathode. When the cathode was cycled/cooled the ratio returned to the nominal value. In Figure 3, both the OX-I and OX-II raw ratios increased slowly as the measurements proceeded and the primary current decreased. Since we did not attempt to adjust the Cs+ focusing as we sputtered away the sample, changes in the bottom surface shape may have introduced small changes to the beam properties which, in turn, caused minor fractionation changes. Alternatively, and perhaps more likely, the slow upward drift of the raw ratios as the measurements proceeded may have been due to a slow drift in the properties of the stripper foil. As we have not seen equivalent differences in raw ratios between samples whose differences in mass caused primary currents to range from 2-7 μA, we do not attribute the slow drift in raw ratios to a direct dependence of measured raw ratio on ion source output. In any case, the slow raw ratio drift appears to have effected all the samples equivalently (implying simple normalization correction), and more importantly from the stand point of routine measurements, there was no appreciable raw ratio drift during the first ~5000 s of sample measurement time (acquisition cycles 1-25).

3d. Efficiency

Based on the data obtained for the 8 samples measured over the three experiments, we calculate a total system efficiency of the CAMS FN-based AMS system for ^{14}C of ~15 %. After corrections for carbon foil stripper charge-exchange efficiency and transmission through the accelerator, and for a small loss on the gridded lens at the entrance to the accelerator, we calculate an ion source C^- ionization efficiency of 25-35% (Table 3).

3e. Efficiency and Sample Size

The benefit to achievable measurement precision provided by a higher efficiency ion source compared to that of less efficient ion sources, given AMS systems with similar transmission and charge exchange characteristics, has been discussed by Ramsey and Hedges [7]. Figure 4 shows the total number of ^{14}C ions expected to reach the detector as a function of OX-I sample mass for a range of ion source efficiencies; the 15% level corresponds to the CAMS ion source and FN-based AMS system, while the lower levels of 1-3% correspond to total system efficiencies that have been quoted for gas ion source based systems [7] and for some Cs sputter ion source based systems which, given typical source efficiencies, stripping efficiencies and transmission loses, would likely fall in the 1-3% total system efficiency range. Figure 4 also shows the measurement uncertainties implied by these numbers of ions reaching the detector based on counting statistics formulations.

In the arena of small (<10 μg C) samples, gas-based ion sources benefit from the elimination of the graphitization step, and its attendant contamination contributions that is required for measurements using solid sample ion sources. However, sample preparation

protocols for both types of ion sources involve steps to convert isolated samples to CO_2 (combustion) and various steps involving chemical and/or physical procedures intended to isolate the sample carbon of interest from other components of the raw samples (pretreatment). The small sample measurement capabilities of any particular ion source/accelerator AMS system will depend, to a significant degree, on the background contaminant contributions of all of the steps leading from raw sample to carbon in the ion source and, in particular, the capabilities will be impacted greatly by the degree to which those contaminants can be identified and controlled.

Assuming the establishment of controls over background contaminant levels that are adequate to reduce their impact on overall small sample capabilities for both gas-based and solid-based ion sources, the significantly higher ionization efficiency of the CAMS ion source will allow the measurement of much smaller samples to a needed level of uncertainty. For instance, examination of Figure 4 shows that the higher efficiency ion source would allow the measurement of 5 μg samples to a counting statistics 1-sigma precision of ±2‰; a system with 1% total system efficiency can only reach that precision for ≥100 μg samples and would be limited to ±30‰ precision for 5 μg samples. Thus, if the sources of background contamination for small samples can be identified and controlled, high-efficiency solid-sample Cs sputter ion sources will have a significant advantage over lower efficiency gas-based ion sources.

4. Summary

The data obtained in this study shows that the modifications made to the CAMS ion sources (increased pumping around sample, uniform Cs heating, 6 jet Cs feed to spherical ionizer, etc.) [1,2] have produced ion sources that operate at both high negative ion output levels (>300 μA $^{12}C^-$) and high negative ion production efficiency. Based on the data obtained in this study, our CAMS/ ion sources operate at ~33% C^- ionization efficiency during routine ^{14}C AMS operations and allow our overall ^{14}C AMS system to operate at a total system efficiency in excess of 15%.

Acknowledgements

We would like to thank Paula Zermeño. and Dot Kurdyla for help preparing graphite targets and Heather Graven (UCSD/SIO) for help during AMS analysis. Thanks to John Southon and an anonymous reviewer for useful comments to the manuscript. This work was performed under the auspices of the U.S. Department of Energy by the University of California, Lawrence Livermore National Laboratory under contract No. W-7405-Eng-48.

References:

1. J.R. Southon, M.L. Roberts, Nucl. Instr. and Meth. 172 (2000).
2. T.A. Brown, M.L. Roberts, J.R. Southon, Nucl. Instr. and Meth. 172 (2000) 344.
3. J.S. Vogel, J.R. Southon, D.E. Nelson Nucl. Instr. and Meth. B29 (1987) 50.
4. I. Karlen, I.U. Olsson, P. Kilburg, S. Kilici, Arkiv Geofysik 4 (1968) 465.
5. W.B. Mann Radiocarbon 25 (2) (1983) 519.

6. J.R. Southon, M.W. Caffee, J.C. Davis, T.L. Moore, I.D. Proctor, B. Schumacher and J.S. Vogel, Nucl. Instr. and Meth. 52 (1990) 301.

7. C.B. Ramsey, R.E.M. Hedges, Nucl. Instr. and Meth. 123 (1997) 539.

Figure Legends

Figure 1. Primary current ($^{13}C^{4+}$ μA) from the 8 samples vs. time (s).

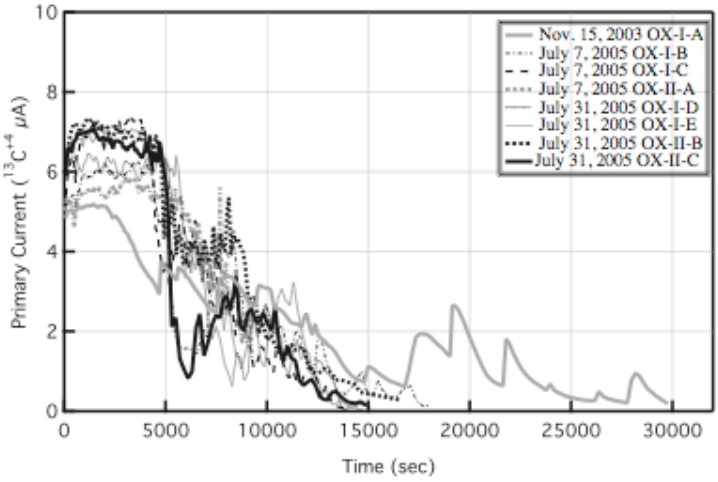

Figure 2. Cumulative ^{14}C gated events (counts) vs. time from the 8 samples. The total number of counts acquired is shown in parentheses in the figure legend.

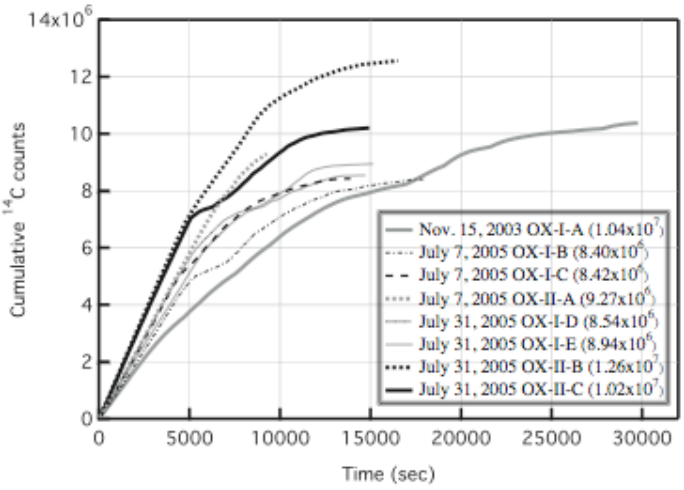

Figure 3. "Raw" ^{14}C counts per nanocoulomb $^{13}C^{4+}$ ratios from the July 7, 2005 experiment.

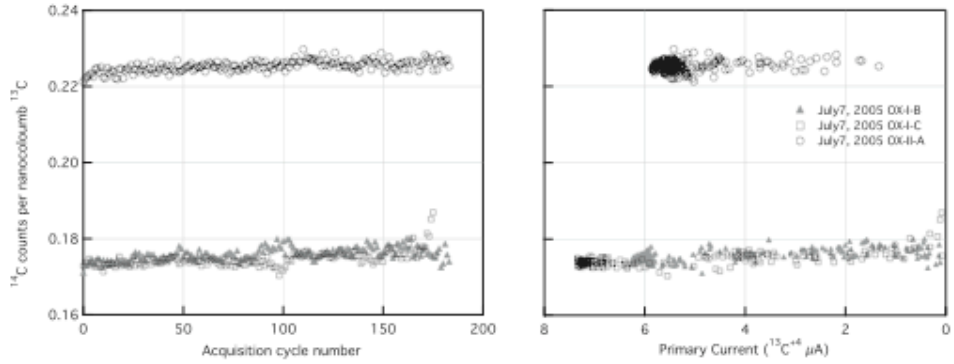

Figure 4. Total ^{14}C counts at the detector (top panel) and the corresponding counting statistics (bottom panel) assuming complete consumption of an OX-I graphite target vs. sample size. The lines correspond to our estimated 15% total efficiency at CAMS, and 3% and 1% overall efficiency. The 3 -5% C^- efficiency quoted for gas ion sources [4] and some sputter based ion sources would, depending upon charge exchange efficiency and transmission losses, likely result in total system efficiencies in the 1-3% range.

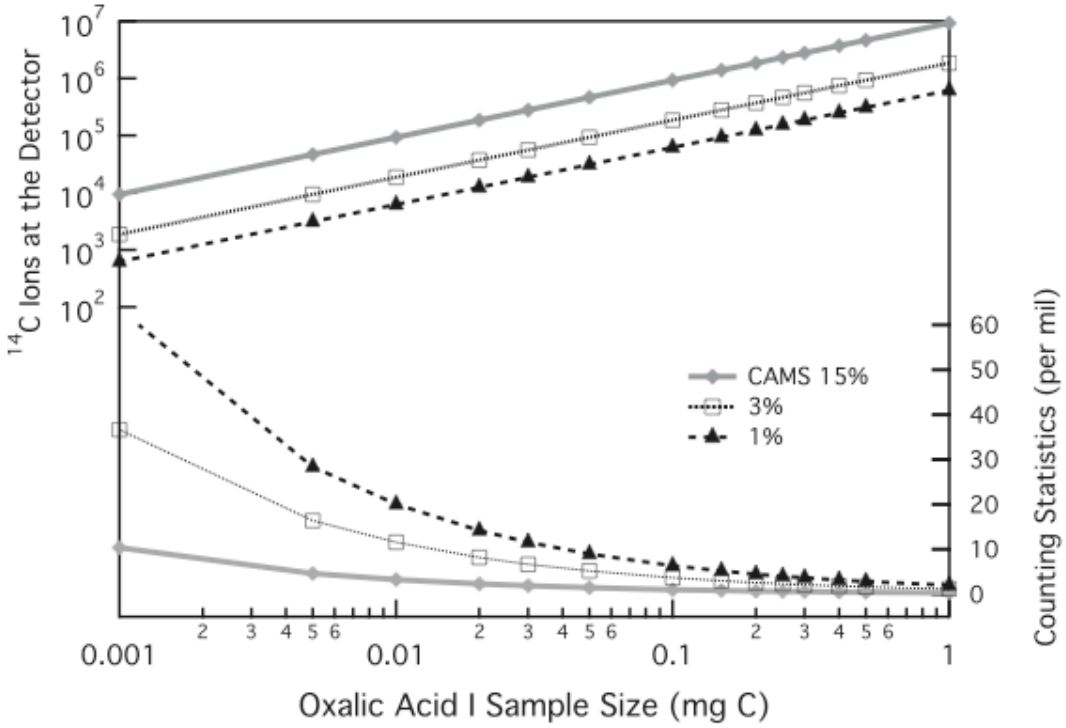
10^7
10^6
10^5
10^4
10^3
10^2
^{14}C Ions at the Detector
CAMS 15%
3%
1%
60
50
40
30
20
10
0
Counting Statistics (per mil)
2 3 4 5 6
0.001
0.01
0.1
1
Oxalic Acid I Sample Size (mg C)

Table 1. CAMS 6.5MeV total transmission efficiency including $^{12}C^-$ to $^{12}C^{4+}$ conversion and a 10% loss at the gridded lens at the entrance to the accelerator.

$^{12}C^-$ Low Energy cup (μA)	$^{12}C^{4+}$ High Energy cup (μA)	Total Transmission Efficiency (%)*
2.23	4.35	48.8
2.18	4.19	48.1
2.18	4.10	47.0
2.18	4.03	45.9
2.17	3.95	45.5
7.25	14.0	48.3
7.10	14.0	49.3
7.06	13.8	49.3
6.95	13.6	48.9
6.85	13.3	48.5
	Average	48.0

- Calculated as conversion = $^{12}C^{4+}/(^{12}C^{-}*4)*100$

Table 2. CAMS Typical Source Operating Settings

Extraction Voltage	40 kV
Cathode Voltage	11.0 kV
Ionizer Power	130 W
Cs Reservoir temperature	Approx. 175 °C
Outputs	250-325 μA $^{12}C^-$ equivalent

Table 3. CAMS Source Efficiency

Sample	^{14}C atoms in target[1]	^{14}C Gated Counts	Total System Efficiency (%)	Ionization Efficiency (%)
Nov. 15, 2003 OX-I-A	62.1×10^6	10.4×10^6	17	35
July 7, 2005 OX-I-B	58.7×10^6	8.4×10^6	14*	29*
July 7, 2005 OX-I-C	58.4×10^6	8.4×10^6	14*	29*
July 7, 2005 OX-II-A	75.5×10^6	9.3×10^6	12*	25*
July 31, 2005 OX-I-D	55.3×10^6	8.5×10^6	15	31
July 31, 2005 OX-1-E	58.5×10^6	8.9×10^6	15	31
July 31, 2005 OX-II-B	75.9×10^6	12.6×10^6	16	34
July 31, 2005 OX-II-C	74.5×10^6	10.2×10^6	14	29

[1]The number of ^{14}C atoms in the targets were calculated from sample size in mg C.
*In the Ionex 846 and similar sources, the sample is cycled in and out of the source for every measurement. The aluminum targets began to break down and get stuck in the ion source after ~170 in/out cycles due to binding caused by aluminum flakes. These targets were not run to exhaustion and thus we can only estimate minimum total system and ionization efficiencies